Surface and interface study on MBE-grown $Nd_{1.85}Ce_{0.15}CuO_4$ thin films by photoemission spectroscopy and tunnel spectroscopy

H. Yamamoto, M. Naito, and H. Sato
NTT Basic Research Laboratories, 3-1 Morinosato-Wakamiya, Atsugi-shi, Kanagawa, 243-01, Japan
(Received 12 August 1996; revised manuscript received 18 February 1997)

$Nd_{1.85}Ce_{0.15}CuO_4$ (NCCO) surfaces and metal (Au, Ag, and Pb)/NCCO interfaces have been extensively investigated by x-ray and ultraviolet photoelectron spectroscopies using films grown by molecular beam epitaxy (MBE). The photoelectron spectra obtained *in situ* on the surfaces of MBE-grown NCCO films are free from any dirt peak and show a fine structure with a Fermi edge in the valence region. Experiments were performed on the prepared clean surfaces, focusing on the evolution of the surface or interface electronic structure with oxygen nonstoichiometry at the surface or interface regions. The results show (1) a systematic spectral change due to the oxygen content at the surface, and (2) a redox phenomena at the metal/NCCO interface. In oxygenated surfaces or insufficiently reduced surfaces, excess oxygens seem to occupy the interstitial (apical) oxygen sites, which compensates Ce doping, eventually leading to a nonmetallic surface. In excessively reduced surfaces, oxygen deficiencies seem to occur at regular oxygen sites, leading to a metallic but not a superconducting surface. The photoelectron spectroscopy data are discussed in comparison with complementary tunnel spectroscopy data. Both sets of data indicate that precise control of oxygen stoichiometry at NCCO surface is essential to obtain an intrinsic (i.e., superconducting) NCCO surface, which is indispensable in obtaining reliable data using surface sensitive experiments and in fabricating tunnel junctions and superlattices with desirable characteristics. [S0163-1829(97)01629-9]

I. INTRODUCTION

Since the discovery of high-transition-temperature superconductors (HTSC's), their electronic structures have been widely studied using surface-sensitive methods such as x-ray photoelectron spectroscopy (XPS), ultraviolet photoelectron spectroscopy (UPS), and electron-energy-loss spectroscopy (EELS). In fact, several review works concerned with HTSC surfaces have already been published.[1–7] However, the importance of the surface study of HTSC's has not been diminished. First, for most HTSC's the standard photoelectron spectra of the ''intrinsic'' surface have not been established. This is mainly because of special difficulty in obtaining bulk-representative surfaces for superconducting cuprates, which generally have the feature that oxygen atoms are loosely bound to the lattice and thereby easily evaporate from the surface. Second, accurate information on the surface and interface seems to be needed to build HTSC-based tunnel junctions, the attempts at which have been unsuccessful in spite of tremendous efforts since the discovery of HTSC's.[8]

NCCO has been extensively investigated by photoemission spectroscopies[6,7,9–27] because its surface is relatively stable among cuprates and also because it belongs to a small family of *n*-type HTSC's.[28,29] A comparison of these with those in the *p*-type family should shed light on the superconducting mechanism of HTSC's. Many experiments on the NCCO surface have been reported, including works on single crystals and single-crystalline films. However, the results are controversial, especially those on the Cu 2*p* spectra, which represent the valence of Cu, namely Cu^{2+} or Cu^{1+} or intermediate between them, and those on the valence-band spectra. We believe, this is mainly because of imperfect surface preparation in the previous works; most of the NCCO surfaces were prepared by filing, fracture, and cleavage. The problems involved in these surface preparation methods were reviewed in a work by Vasquez.[6]

In order to prepare clean surfaces of NCCO, we used molecular beam epitaxy (MBE) in this work. We can grow NCCO superconducting films with a smooth surface, having good electrical and superconducting properties by the precise stoichiometry control of the constituent cations in MBE.[30–32] The photoemission spectra obtained *in situ* on the surface of MBE-grown NCCO films are free from any dirt peaks, and show a fine structure and a Fermi edge in the valence-band region. Furthermore, it has been established that the spectra obtained using these films are reproducible. Extensive measurements of XPS and UPS have been performed on the thusly prepared clean surfaces. Some tunnel spectroscopy measurements have also been made to support and complement the photoemission data. Our experiments have focused on the following points: (1) the evolution of the surface electronic structure with oxygen nonstoichiometry at the surface and the identification of the photoemission spectra of the bulk-representative (i.e., superconducting) NCCO surface; and (2) the effect of oxygen transfer (redox reaction) at metal/NCCO interfaces.

The results indicate the surface and interface electronic structures of NCCO are strongly influenced by oxygen nonstoichiometry, and that the precise control of oxygen content at the surface (interface) region is essential to obtain the bulk-representative surface (interface). This is because the surface or interface region is directly exposed to the environment, and hence oxygen non-stoichiometry can be produced more easily than inside the bulk. These consequences mean we should exercise extreme caution in investigating HTSC's using surface-sensitive spectroscopies such as angle-resolved photoemission spectroscopy and scanning tunnelling spec-

troscopy, and in fabricating HTSC-based tunnel junctions and superlattices.

This paper is organized as follows. Section II describes the experimental aspects of this work, including MBE growth of NCCO films, XPS and UPS measurements, and tunneling measurements. Section III presents and discusses the results. In Sec. III A, the surfaces of as-grown NCCO films, which are reduced in various conditions or oxygenated, are compared, and it is argued from the results with an aid of resistivity data and tunnel spectra which surface will be ''intrinsic.'' In Sec. III B metal/NCCO interfaces are investigated by photoemission and tunnel spectroscopies. We examine metals such as Au, Ag, and Pb, which are widely used as counter electrodes of SIN tunnel junctions and contact electrodes. For Pb, evidence of formation of PbO_x/oxygen-depleted NCCO complexes in *in situ* junction by interface reaction is presented and the way to prevent it is proposed. Section IV is a brief summary.

II. EXPERIMENT

A. MBE growth of NCCO films

The films were grown in a custom-designed UHV chamber (chamber base pressure $\sim 10^{-9}$ Torr) equipped with multiple electron gun evaporators, whose details were described elsewhere.[33] Substrates used for surface analyses were (001) Nb(0.5%)-doped $SrTiO_3$ (conductive) and those used for electrical and tunnel measurements were undoped $SrTiO_3$ (insulating).[34] The substrate temperature measured by an infrared pyrometer was 730 ± 10 °C. As oxidation gas, 1–1.5 sccm of ozone gas (not distilled, 5–10 % ozone concentration) was supplied through an alumina tube directed at the substrate at a distance of 1–2 cm. The total deposition rate was ~0.15 nm/sec, and the film thickness was 100 nm. It was confirmed by x-ray diffraction and reflection high-energy electron diffraction (RHEED) that all of the NCCO films were single phased and *c*-axis oriented. The doping concentration of Ce was optimized, i.e., the film composition was assumed to be roughly $Nd_{1.85}Ce_{0.15}CuO_4$. These films, if they are properly reduced, typically show $T_c^{\rm end} = 22-23$ K, $\rho(300\ {\rm K}) = 150-200\ \mu\Omega$ cm, and $\rho(30\ {\rm K}) = 30-40\ \mu\Omega$ cm. These values are better than the best reported for single crystals.[35]

After deposition, in order to avoid phase decomposition of film surface, ozone gas was supplied until the films cooled down to ~630 °C. The ozone gas supply was then cut, and the films were cooled down to ambient temperature (~200 °C) in various reducing conditions. This reduction cooldown process has so far been made not along the isocomposition line (constant δ of $Nd_{1.85}Ce_{0.15}CuO_{4-\delta}$),[36] but under constant partial pressure (P_{O_2}) of molecular oxygen. The reason is mainly the experimental limitation that the diffusion of oxygen is too slow at low temperatures for one to follow the isocomposition line exactly.[37,38] Specifically, under constant P_{O_2}, films were kept at ~630 °C for 600 sec and cooled down to ambient temperature at the rate of ~20 °C/min. The P_{O_2} in reduction was varied from $\leq 10^{-8}$ Torr to 3×10^{-5} Torr by controlling the flow of molecular oxygen introduced into the chamber from 0 sccm to 1 sccm.[39] In this work, for convenience, P_{O_2}, is mostly denoted by the oxygen flow, which gives $P_{O_2} = 3.5 \times 10^{-5}$ Torr per 1 sccm O_2 flow. For the purpose of comparison, we also made a few oxygenated films, which were cooled down with the same amount of ozone gas supply as during growth.

B. Characterization of NCCO surface and metal/NCCO interface by XPS and UPS

For *in situ* surface analysis by XPS and UPS, grown films were transferred *in vacuo* to an analysis chamber with a base pressure of $\sim 3\times10^{-10}$ Torr. Unmonochromatized Mg $K\alpha$ and Al $K\alpha$ (VG XR3E2) and He I, He II (VG UVL-HI) were used as x-ray and ultraviolet sources, and CLAM2 (VG) was used as an electron energy analyzer.

For characterization of *in situ* metal/NCCO interfaces, a 1.0-nm-thick metal (Au, Ag, Pb) was deposited on an as-grown NCCO surface at a substrate temperature of 100–150 °C in the growth chamber. Judging by RHEED, streaky diffraction patterns from NCCO fade away completely with this metal deposition, indicating that the entire surface of NCCO was covered with the metal. The prepared metal/NCCO specimens were transferred *in vacuo* to the analysis chamber for XPS and UPS investigations. *Ex situ* fabricated Pb/NCCO interfaces, where Pb was deposited on NCCO surfaces after exposed to 0.2 atm of pure O_2 or air, were also examined to elucidate the difference in tunnel spectra described below.

C. Tunnel junction fabrication

Two types of tunnel junctions were fabricated: *in situ* and *ex situ*. In *in situ* junction fabrication, metal counter electrodes (~50 nm) were deposited on as-grown NCCO film at a substrate temperature of 100–150 °C in the growth chamber. Junctions were fabricated by an ordinary photolithographic process. The junction area is typically between 0.1 mm×0.1 mm and 0.4 mm×0.4 mm. In *ex situ* junction fabrication, films were taken out of the growth chamber, and 10–20 days later they were coated with polystyrene *Q*-dope except for a narrow strip 0.2–0.5 mm in width. Then counter electrodes (Pb, Au, etc.) of ~0.2 mm wide cross strips were evaporated in a bell jar.

III. RESULTS AND DISCUSSION

A. Surface of as-grown NCCO films

1. ρ-T characteristics of the NCCO films

Figure 1 shows the temperature dependence of the resistivity of NCCO films that were reduced under various P_{O_2} or oxygenated in O_2+O_3. In the reduced films, the overall behavior of resistivity does not change with P_{O_2} very much, except that the low-temperature resistivity increases and T_c decreases slightly with increasing P_{O_2}. On the other hand, as shown below, the surface structure and surface electronic structure change significantly with P_{O_2}. This fact indicates that the surface structure and surface electronic structure of the films do not represent inner structure and inner electronic structure of the films. This problem seems to be due to our reduction process, which does not follow the isocomposition

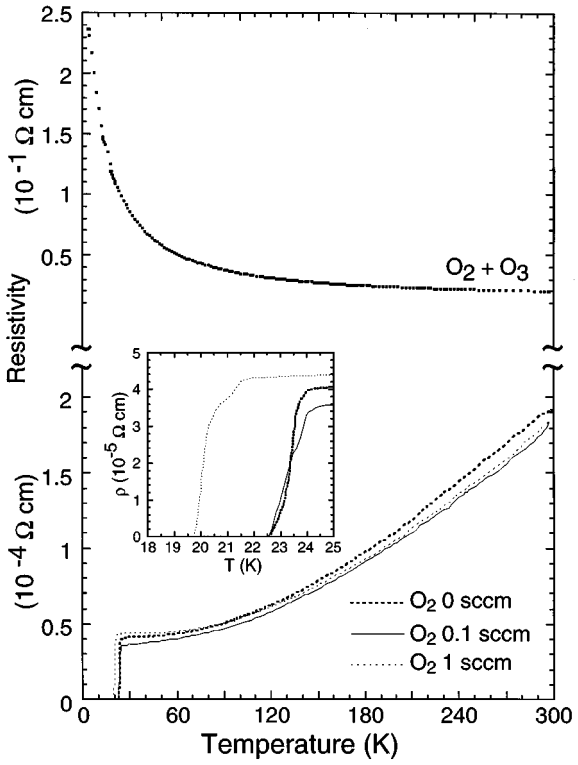

FIG. 1. Resistivity ρ vs temperature T for NCCO reduced in various P_{O_2} or oxygenated. Inset: ρ vs T around the superconducting transition.

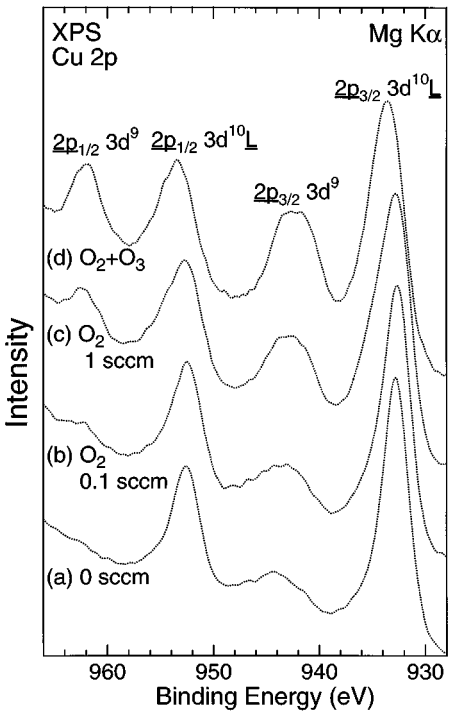

FIG. 2. *In situ* Cu $2p$ XP spectra of NCCO films reduced in (a) 0, (b) 0.1, (c) 1 sccm O_2, and (d) oxygenated in O_2+O_3. Parameters related to the position, width, and intensity of the peaks are summarized in Table I.

line.[36] Sluggish oxygen diffusion at low temperatures[37,38] causes an inhomogeneous oxygen concentration to develop in the depth direction. In insufficient reduction, the oxygen concentration should be higher toward surface, whereas in excessive reduction, the oxygen concentration should be lower toward surface. Fairly homogeneous oxygen concentration can be obtained only when optimal reduction is made. The resistivity of an oxygenated film, which is also shown in Fig. 1, is 3 orders of magnitude higher at room temperature and exhibits semiconducting behavior.

2. Results of Cu 2p XPS and valence UPS

Figure 2 shows the *in situ* Cu $2p$ XP spectra of the above NCCO films. These spectra are raw data without subtraction of components from Mg $K\alpha'$, $K\alpha_3$, etc. The conventional notation such as $\underline{2p_{3/2}}3d^{10}\underline{L}$ [L; ligand (oxygen)], $\underline{2p_{3/2}}3d^9$ is given to each peak. For convenience, we call $\underline{2p}3\overline{d^{10}}\underline{L}$ the main peak and $\underline{2p}3\overline{d^9}$ the satellite peak, and the $\overline{\text{ }}$ notation of I_s/I_m is used to express the intensity ratio of these peaks hereafter. Table I summarizes the binding energies (BE's) and the full widths at half maximum (FWHM's) of the peaks, the energy separations (W's) between the main peak and the satellite peak, and the I_s/I_m ratios. For I_s/I_m, we used the ratio of the Cu $2p_{1/2}$ satellite peak to the Cu $2p_{1/2}$ main peak because this minimizes the influence of $K\alpha'$, $K\alpha_3$, etc., which have higher photon energies than $K\alpha$ and give spurious intensity at the position of Cu $\underline{2p_{3/2}}3\overline{d^9}$. The energy separation W is related to the Coulomb repulsive energy between a Cu $2p$ electron and a Cu $3d$ electron. The I_s/I_m ratio increases with increasing P_{O_2} in reduction. This change in I_s/I_m corresponds to a change in the valence of Cu. Namely, the valence of Cu at a surface, which is intermediate between $+1$ and $+2$, comes closer to $+2$ with increasing P_{O_2}. For the film reduced in a 0 sccm O_2, I_s/I_m is very small, indicating that Cu at the surface is close to monovalent. The FWHM of the main peak also increases with increasing P_{O_2}. The I_s/I_m ratio is enlarged further in the oxygenated film. The FWHM of the main peak of the oxygenated film is nearly equal to that of the film reduced in 1 sccm O_2, although the detailed shape is different. The peak energy of the main peak also has a higher binding energy in the oxygenated film.

Figure 3 shows the corresponding valence UP spectra. The ultraviolet source was He I (21.2 eV) for spectra $(a)-(d)$ and He II (40.8 eV) for spectra $(a')-(d')$. The UP spectra show negligible intensity for the so-called 9-eV dirt peak,[2,40,41] reconfirming that the surface of our sample is free from contaminants. Furthermore, the UP spectra show a Fermi edge for the reduced films $[(a)-(c),(a')-(c')]$ and also a fine structure in the valence-band region around 2–7 eV. Suzuki *et al.*[16] pointed out that, for the cleaved surface of an NCCO polycrystalline pellet, the Fermi edge can be observed in XPS but not in UPS despite the advantage of UPS in imaging photoionization cross sections,[42] and explained that this is because XPS has a more probing depth than UPS and therefore is able to detect a deeper and more intrinsic region inside specimens even if a few top layers are degraded. In addition, only a few groups have succeeded in observing the Fermi edge of NCCO using photons with $h\nu = 35-75$ eV (Refs. 17, 18, 24, and 25) or $h\nu = 17$ eV (Ref. 25) prepared by synchrotron radiation. In one case, $h\nu$

TABLE I. Position (E_B), full width at half maximum (FWHM), energy separation (W), and intensity ratio (I_s/I_m) of Cu $2p_{1/2}$ obtained from the Cu $2p$ XPS spectra. W is defined as the difference between E_B of satellite and that of main.

	Cu $2p_{3/2}$ main		Cu $2p_{3/2}$ sat.			Cu $2p_{1/2}$ main		Cu $2p_{1/2}$ sat.			$\frac{I_s(\text{Cu } 2p_{1/2})}{I_m(\text{Cu } 2p_{1/2})}$
Oxygen supply	E_B (eV)	FWHM (eV)	E_B (eV)	FWHM (eV)	W (eV)	E_B (eV)	FWHM (eV)	E_B (eV)	FWHM (eV)	W (eV)	
Vacuum	932.8	1.5	943.7	2.1	10.9	952.6	1.6	—	—	—	~0
O_2 0.1 sccm	932.7	1.6	943.3	2.2	10.6	952.4	1.9	962.7	(1.9)	10.3	0.14
O_2 1 sccm	932.8	2.2	942.7	2.3	9.9	952.7	2.2	962.4	(2.2)	9.7	0.36
O_2+O_3	933.7	2.0	942.2	3.3[a]	8.5	953.4	2.0	962.0	(2.0)	8.6	0.55

[a]If the Cu $2p_{3/2}$ satellite peak in Fig. 2 (d) consists of a single component.

$=16.8$ eV by Ne I.[26] Our MBE-grown films show the Fermi edge in conventional He(I) and He(II) UPS, presenting more evidence of the high quality of the surfaces and that the films are metallic up to the surface. In the valence-band region, the spectrum shapes of the spectra with He(I) and with He(II) are different. The peaks observed in He(I) UP spectra are not always observed in He(II) UP spectra (e.g., peaks B,β), and *vice versa* (e.g., peaks A', δ'). Here, each peak in He(II) UP spectra is labeled by a letter with a prime. Peak D and peak γ' seem to have different origins for reasons described below, although their position is the same. The peak positions are summarized in Table II.

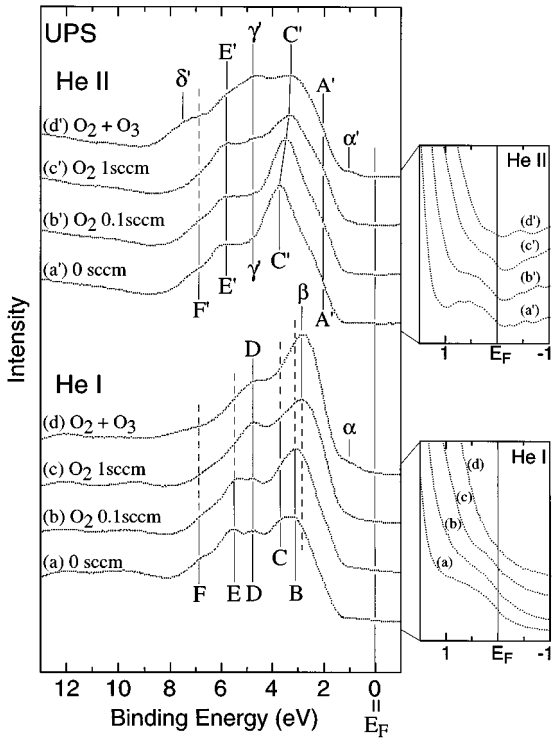

FIG. 3. *In situ* valence UP spectra of NCCO films reduced in $(a),(a')$ 0 sccm, $(b),(b')$ 0.1 sccm, $(c),(c')$ 1 sccm O_2, and $(d),(d')$ oxygenated. The ultraviolet source was He(I) for the spectra $(a)-(d)$ or He(II) for the spectra $(a')-(d')$. Each peak in the He(II) UP spectra is labeled by a letter with a prime. The peaks $B-F$ and A', C', E' F' are due to the intrinsic energy bands, whereas the peaks α, β, and α', γ', δ' are due to extrinsic orbitals (see text). Their peak positions are summarized in Table II. A Fermi edge is observed except in $(d),(d')$. Fine structures around 2–7 eV are observed for all the films. The so-called 9 eV structure with extrinsic origin (Refs. 2, 40, 41) has negligible intensity in all spectra.

3. Discussion

The above results are discussed here in connection with the role of oxygen nonstoichiometry at the surface. First, the Cu $2p$ spectra will be discussed. Parmigiani *et al.*[23] pointed out that the main Cu $2p_{3/2}$ XPS core line in Nd_2CuO_4, where the Cu^{2+} ions are coordinated by four O^{2-} ions in a square planar configuration, is narrower than that in La_2CuO_4 with the Cu^{2+} coordinated by six O^{2-} ions in an octahedral configuration. We confirmed this by comparing our NCCO and preliminary LSCO spectra. Parmigiani *et al.* explained that the difference in the $2p_{3/2}$ line width between these two configurations is caused by a difference in the charge transfer mechanism; in the square planar configuration, only the O $p_{x,y}\rightarrow$Cu $d_{x^2-y^2}$ charge-transfer mechanism can take place, whereas in the octahedral configuration, O $p_z\rightarrow$Cu d_{z^2} as well as O $p_{x,y}\rightarrow$Cu $d_{x^2-y^2}$ is allowed, and hence these two different configurations will produce different ionization potentials for the Cu $2p_{3/2}$ core level.

The Cu $2p$ spectrum of the oxygenated NCCO film is close to our preliminary Cu $2p$ spectrum of an LSCO film in that both show a large I_s/I_m ratio and a wide $2p_{3/2}$ main line. This indicates that a fair amount of excess oxygen atoms probably occupy interstitial sites [O(3)], which correspond to the apical sites of the related T structure.[43] The semiconducting behavior of the resistivity of the oxygenated film suggests that oxygen atoms also occupy apical sites well inside the film, at least partially. This picture seems to be consistent with the recent neutron-diffraction results,[44,45] the EXAFS results,[46] and also the early TGA results[47] on $Nd_2CuO_{4+\delta}$ and $Nd_{2-x}Ce_xCuO_{4+\delta}$. The surface of NCCO reduced in 1 sccm O_2 also shows a similar tendency, to a less pronounced degree, in the Cu $2p$ spectrum, indicating the reduction is insufficient. The occupancy of the apical sites at the surface in this film will be somewhat lower than in the oxygenated film. Moreover, this occupancy seems to occur mainly in the limited region near the surface, with an extremely small percentage inside the film, as suggested from the resistivity data.

It is not easy to decide which of those reduced in 0 or in 0.1 sccm O_2 is an intrinsic (i.e., superconducting) surface since the films reduced in 0 and 0.1 sccm O_2 show a differ-

TABLE II. Position of the peaks observed in UP spectra in Fig. 3.

		Intrinsic						Extrinsic			
He I	Peak	A	B	C	D	E	F	α	β	γ	δ
	Position (eV)	-	3.1	3.7	4.8	5.5	6.9	1.0	2.8	-	-
He II	Peak	A'	B'	C'	D'	E'	F'	α'	β'	γ'	δ'
	Position (eV)	2.0	-	3.3 $\sim$3.7	-	5.8	6.9	1.0	-	4.8	7.5

ence only in the I_s/I_m ratio. The results are essentially identical for the rest, including the valence-band spectrum, the resistivity, and the RHEED pattern.[48] Nevertheless, we adopt the surface reduced in 0.1 sccm O_2 as representing the ''intrinsic'' surface of NCCO. This conclusion is based on our preliminary tunnel experiments indicating that the Cu^{1+} surface is metallic, but not superconducting. The reduction in 0 sccm O_2 seems to be excessive. Several neutron-diffraction experiments have indicated deficiencies of both O(1) in the CuO_2 plane and O(2) in the Nd_2O_2 plane in excessively reduced $Nd_2CuO_{4-\delta}$ (Refs. 44 and 49) and $Nd_{1.85}Ce_{0.15}CuO_{4-\delta}$.[45] The deficiency of either site changes the doping level from optimum to overdoped. Furthermore, the deficiency of O(1) sites disrupts the network in the CuO_2 planes, which may have a more fatal effect on superconductivity. At present, we cannot determine whether it is O(1) or O(2) that is dominantly deficient at excessively reduced (i.e., reduced in 0 sccm O_2) surfaces.

Next, the valence-band spectra are discussed on the basis of the above picture of oxygen nonstoichiometry at the surface. The peaks $B-F$ and A', C', E', F' seem to be due to the intrinsic energy bands of the bulk T' crystal structure, whereas the peaks α, β, and α', γ', δ' seem to be due to extrinsic states. It is assumed that, in the film reduced under high P_{O_2} and in the oxygenated film, oxygen occupancy at apical sites should modify the Cu $3d_{z^2}$ states to the Cu $3d_{z^2}$-O $2p_z$ $dp\sigma$ states at the NCCO surface. The extrinsic peaks are considered to be derived from this Cu $3d_{z^2}$-O $2p_z$ $dp\sigma$ orbital. Therefore, the intensity of an intrinsic peak should either decrease or not change with P_{O_2}, whereas the intensity of an extrinsic peak should increase with increasing P_{O_2} and become maximum in the oxygenated film. From the intensity change, the peak D and the peak γ' have a different origin despite their having the same energy position, i.e., peak D is intrinsic whereas peak γ' is extrinsic. The intrinsic peaks have some correspondence with the spectrum obtained by Sakisaka *et al.*[17] They measured valence-band photoemission spectra (not *in situ*) as a function of the energy of the incident photon (25–90 eV) for a NCCO film with $T_c \sim 12.5$ K. Our peaks C, C', and D appear to correspond to their 3.6 and 5.0 eV peaks, respectively, and furthermore our small peaks A', F, and F' to their 1.9 and 7.1 eV peaks. Sakisaka *et al.* concluded that the 3.6 eV peak is dominated by Cu $3d$ states and the 5.0 eV peak by O $2p$ states from the energy dependence of the spectrum shape. Our observation also supports their conclusion. According to the calculated atomic ionization cross-section table,[42] the cross-section ratio of atomic Cu $3d$ and O $2p$ $[\sigma(\text{Cu } 3d)/\sigma(\text{O } 2p)]$ is larger for He(II) than for He(I) by a factor of roughly 2. Peaks C' in (a'),(b') in the He(II) UP spectra is more apparent than peak C in (a),(b) in the He(I) spectra in Fig. 6, whereas peak D is more apparent in the He(I) spectra. A detailed description of the valence-band structures including the Ce-doping dependences will be reported elsewhere. All that should be emphasized here is the valence-band spectra or the electronic structures change significantly with the oxygen content near the surface region.

B. Metal/NCCO interface

First, the Cu $2p$ XP spectra for *in situ* metal/NCCO interfaces will be discussed. Figure 4, $(a)-(c)$, shows the Cu $2p$ XP spectra for the *in situ* surface of the optimally reduced NCCO film (a), Au (1.0 nm)/NCCO interface (b), and Pb (1.0 nm)/NCCO interface (c). Both spectra (b) and (c) were obtained after *in situ* deposition of the corresponding metals on the ''intrinsic'' NCCO surface. Although the background shapes in spectra (a), (b), and (c) are different from one another, it is noticed from the comparison with spectrum (a) that, the I_s/I_m ratio does not change in the Au/NCCO interface, while this ratio apparently diminishes in the Pb/NCCO interface. This implies that a reduction of NCCO by Pb occurs at the Pb/NCCO interface. We also examined the interface between Ag and NCCO. The result on Ag is essentially identical to that on Au. The corresponding Au $4f$ and Pb $4f$ XP spectra are shown in Figs. 5(a) and 5(b), which provide complementary information on the metal/NCCO interfaces. In the Au/NCCO interface, Au $4f_{7/2}$ and $4f_{5/2}$ have single peaks. On the contrary, in the Pb/NCCO interface, Pb $4f_{7/2}$ and $4f_{5/2}$ have two components: one that originates from metallic Pb and another from a Pb oxide, indicating the presence of PbO_x in the interface region. These results indicate that the deposition of a metal on NCCO, depending on the reactivity of the metal to oxygen, causes reduction of the NCCO surface and concomitant oxidization of the metal. For Au and Ag, hardly any reaction occurs with NCCO. On the other hand, even for Pb, which is supposed to have moderate reactivity to oxygen, redox reaction occurs with NCCO, leading to the formation of PbO_x/oxygen-depleted NCCO interface complexes.

Next, we shall discuss the Pb/NCCO interface prepared in various conditions. Spectra (d) and (e) in Fig. 4 were obtained after Pb deposition on the 0.2-atm pure-O_2 exposed surface (d) and on air-exposed surface (e) of optimally reduced NCCO films. Figure 4 also shows the corresponding Cu $2p$ XP spectra of the 0.2-atm pure-O_2 exposed surface (f) and air-exposed NCCO surface (g) *before* depositing Pb

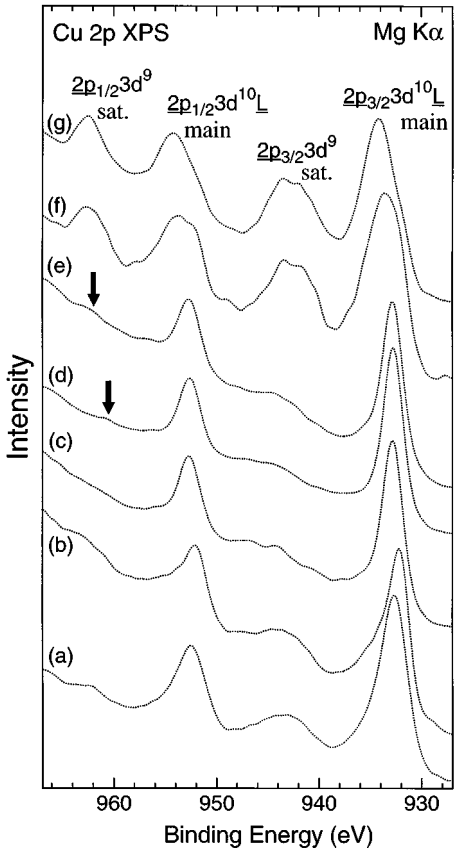

FIG. 4. Cu $2p$ XP spectra for (a) the *in situ* surface of the optimally reduced NCCO film (''intrinsic'' surface), (b) the *in situ* Au (1.0 nm)/NCCO interface, (c) the *in situ* Pb (1.0 nm)/NCCO interface, (d) the *ex situ* Pb (1.0 nm)/0.2-atm O_2-exposed NCCO interface, (e) the *ex situ* Pb (1.0 nm)/air-exposed NCCO interface, (f) the 0.2-atm O_2-exposed NCCO surface, and (g) the air-exposed NCCO surface.

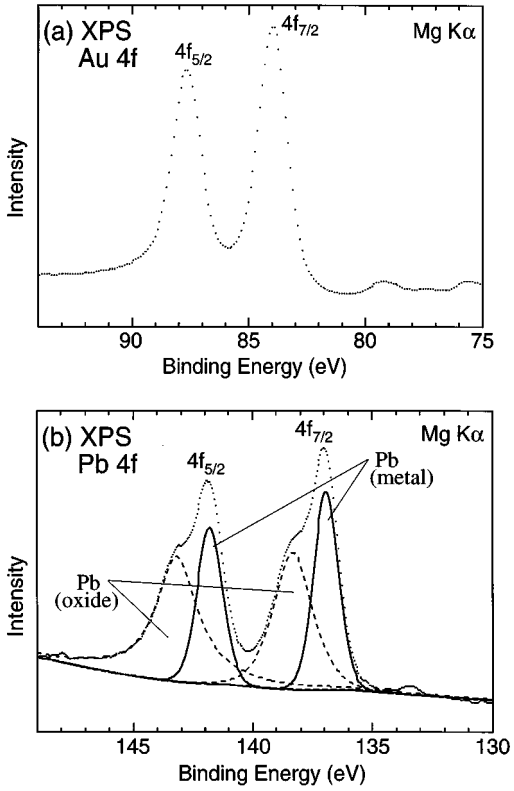

FIG. 5. Au $4f$ (a) and Pb $4f$ (b) XP spectra obtained from the *in situ* Au/NCCO interface and the *in situ* Pb/NCCO interface, respectively. The Au $4f$ peak consists of a single peak, whereas the Pb $4f$ consists of two components of metallic Pb and Pb oxide.

on them. Oxygen exposure distinctly enlarges the I_s/I_m ratio and makes the Cu $2p$ main line broaden and shift to higher binding energy $[(f)]$, indicating the adsorption of oxygen at the surface: a fair amount of excess oxygen occupies interstitial apical sites [O(3)]. Further exposure to air for a long time (up to 2 weeks) brings about no essential change in the Cu $2p$ XP spectrum $[(g)]$, although some evidence of H_2O/CO_2 adsorption is seen in O $1s$ XP spectra and valence spectra. The detailed description of stability of the NCCO surface against air will be given elsewhere.[50] For all of the surfaces shown in $(c)-(e)$, Pb deposition apparently diminishes the I_s/I_m ratio, indicating the occurrence of redox reaction between Pb and NCCO. The valence of Cu in (c) is close to $+1(I_s/I_m \sim 0)$, indicating oxygen deficiencies at the regular sites [O(1) and/or O(2)]. On the other hand, the Cu $2p_{1/2}$ satellite peak has weak but finite intensity in (d) and (e); i.e., the Cu valence in (d) and (e) is intermediate between $+1$ and $+2$. This suggests that oxygen and H_2O/CO_2 adsorption protects, to some extent, NCCO from suffering from oxygen deficiencies at the regular site by Pb deposition.

Complementary results were obtained from the Pb/NCCO tunnel spectra. Figure 6 shows the dI/dV characteristics of Pb/NCCO tunnel junctions fabricated by the *in situ* $[(a),(a')]$ and *ex situ* $[(b),(b')]$ processes using optimally reduced NCCO films. The solid lines $[(a)$ and $(b)]$ represent the data taken at $T=9$ K, where Pb is normal and the broken lines $[(a')$ and $(b')]$ the data taken at $T<1.4$ K, where Pb is superconducting. In either junction, the dominant electron transport process seems to be elastic tunneling since the superconducting gap and the phonon structure of Pb are observed clearly at $T<1.4$ K. However, the superconducting gap structure of NCCO is hardly observed at all in the *in situ* tunnel junction. The superconductivity of NCCO is completely lost in the *in situ* Pb/NCCO junction due to oxygen depletion in the interface region. On the other hand, in the *ex situ* junction the oxygen deficiencies at the regular sites seem to be significantly suppressed. The superconducting gap structure of NCCO with a reasonable gap value (~ 4 meV) (Ref. 51) can be clearly seen in the *ex situ* junction. However, the high zero-bias conductance ($\sim 20\%$ of the normal conductance at our best) and the smeared shape of dI/dV indicate the presence of a normal-metal region and the distribution of the magnitude of the superconducting gap. This seems to be caused by a nonuniform oxygen distribution at the interface.

In connection with the above metal/NCCO reaction at the interface, it should be noted that the conventional amorphous metal-oxide barriers for metallic or intermetallic superconductors will not work for high-T_c cuprates to fabricate tunnel junctions. We have tried CeO_2 and Al_2O_3 barriers on NCCO by depositing Ce or Al at ambient temperature and subsequently oxidizing them. The junctions with these barriers

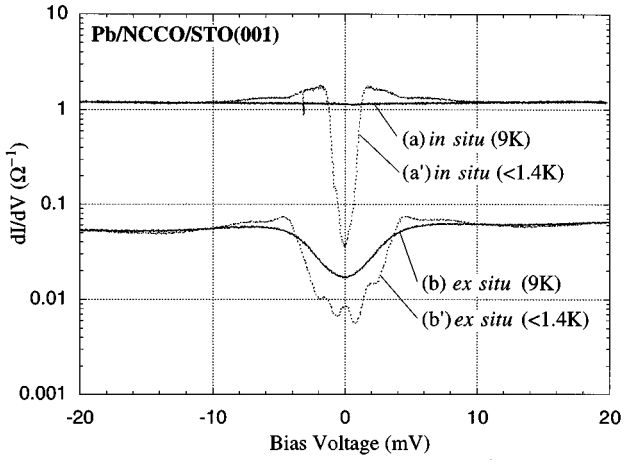

FIG. 6. Conductance curves for *in situ* $[(a),(a')]$ and *ex situ* $[(b),(b')]$ Pb/native barrier/NCCO tunnel junctions fabricated by using the optimally reduced NCCO films. Spectra (a) and (b) were measured at $T=9$ K (i.e., Pb is nonsuperconducting), whereas spectra (a') and (b') were measured at $T<1.4$ K (i.e., Pb is superconducting). The superconducting gap structure of NCCO is clearly observed in spectrum (b) and (b'), whereas it is hardly observed at all in (a) and (a'). The additional fine structures observed in (a') and (b') are due to the superconducting gap and the phonon structure of Pb. A zero bias peak is also observed in (b') whose origin is unknown. It should also be noted that the tunnel conductance is significantly higher in the *in situ* junction than in the *ex situ* junction.

exhibited very high resistance and no superconducting gap structure of NCCO, which indicates that a reaction similar to that in the Pb/NCCO interface occurs to a more serious extent.

IV. SUMMARY

We have extensively investigated NCCO surfaces and metal/NCCO interfaces by x-ray and ultraviolet photoelectron spectroscopies and tunnel spectroscopy using films grown by MBE. The results are summarized as follows.

(1) *In situ* photoelectron spectroscopies on well-controlled MBE-grown films provide one of the best opportunities for studying the intrinsic surfaces of high-T_c cuprates. The photoelectron spectra obtained *in situ* in the present study are free from any dirt peaks and show a fine structure with a Fermi edge in the valence-band region.

(2) The intrinsic surface of superconducting $Nd_{1.85}Ce_{0.15}CuO_4$ was identified. The NCCO surface shows a systematic change in the Cu $2p$ XP spectrum with changing oxygen content near the surface. The Cu $2p$ XPS shows that Cu at the surface changes from divalentlike for insufficient reduction ($P_{O_2}\geqslant 10^{-5}$ Torr) to monovalentlike for excessive reduction ($P_{O_2}\leqslant 10^{-8}$ Torr). The intrinsic surface of superconducting $Nd_{1.85}Ce_{0.15}CuO_4$ can be obtained only by the optimum reduction ($P_{O_2}=1\sim 5\times 10^{-6}$). These spectra can be used as the indices whether a surface prepared by a researcher is intrinsic or not. With insufficient reduction, excess oxygen atoms seem to occupy interstitial apical sites [O(3)], which compensates the Ce doping, eventually leading to nonmetallic surface. On the other hand, with excessive reduction, oxygen deficiencies seem to occur at regular sites [O(1) and/or O(2)], leading to a metallic but not a superconducting surface.

(3) The valence-band UP spectrum also changes with varying reduction conditions. The change is significant with insufficient reduction, but small with excessive reduction. The spectral change in the valence band of the NCCO surface with insufficient reduction seems to originate from the modification of the Cu $3d_{z^2}$ states into the Cu $3d_{z^2}$-O $2p_z$ $dp\sigma$ states due to oxygen occupying apical sites.

(4) The metal/NCCO interfaces have been investigated by XPS and tunnel spectroscopy. For Au and Ag, no reaction occurs with NCCO. For reactive metals such as Pb, however, redox reaction occurs, leading to the formation of metal-oxide–oxygen-depleted NCCO interface complexes if Pb is deposited *in situ* on NCCO. This reaction destroys the superconductivity of NCCO at the interface region. This problem may be universal in cuprate and any spectra of high-T_c tunnel junctions may suffer from this problem. This redox phenomena is considered to be the intrinsic reason why attempts to fabricate high-T_c tunnel junctions have been unsuccessful.

These results strongly indicate that precise control of oxygen content of the NCCO surface is essential to obtain an intrinsic (i.e., superconducting) NCCO surface, which is indispensable in obtaining reliable data in surface-sensitive experiments and also in fabricating tunnel junctions and superlattices with desirable characteristics.

ACKNOWLEDGMENTS

The authors would like to acknowledge valuable comments from Dr. N. Terada of the Electrotechnical Laboratory. We are also grateful to Dr. A. Matsuda and Dr. T. Yamada for their helpful discussions, and Dr. N. Matsumoto, Dr. T. Ikegami, and Dr. T. Izawa for their support and encouragement.

[1] H. M. Meyer III and J. H. Weaver, in *Physical Properties of High Temperature Superconductors II*, edited by D. M. Ginsberg (World Scientific, Singapore, 1990), p. 369, and references therein.

[2] P. A. P. Lindberg, Z.-X. Shen, W. E. Spicer, and I. Lindau, Surf. Sci. Rep. **11**, 1 (1990).

[3] F. A. Shamma and J. C. Fuggle, Physica C **169**, 325 (1990).

[4] B. W. Veal, R. Liu, A. P. Paulikas, D. D. Koelling, H. Shi, J. W. Downey, C. G. Olson, A. J. Arko, J. J. Joyce, and R. Blythe, Surf. Sci. Rep. **19**, 121 (1993).

[5] C. R. Brundle and D. E. Fowler, Surf. Sci. Rep. **19**, 143 (1993).

[6] *Spectroscopy and High Temperature Superconductors–The Current Understanding of High Temperature Superconductors Revealed by Spectroscopy*, edited by R. P. Vasquez (Elsevier, Amsterdam, 1994).

[7] Z.-X. Shen and D. S. Dessau, Phys. Rep. **253**, 1 (1995).

[8] T. Hasegawa, H. Ikuta, and K. Kitazawa, in *Physical Properties of High Temperature Superconductors III*, edited by D. M. Ginsberg (World Scientific, Singapore, 1992), p. 525, and references therein.
[9] M. K. Rajumon, D. D. Sarma, R. Vijayaraghavan, and C. N. R. Rao, Solid State Commun. **70**, 875 (1989).
[10] S. Uji, M. Shimoda, and H. Aoki, Jpn. J. Appl. Phys. **28**, L804 (1989).
[11] H. Ishi, T. Koshizawa, H. Kataura, T. Hanyu, H. Takai, K. Mizoguchi, K. Kume, I. Shiozaki, and S. Yamaguchi, Jpn. J. Appl. Phys. **28**, L1952 (1989).
[12] Y. Fukuda, T. Suzuki, M. Nagoshi, Y. Syono, K. Oh-ishi, and M. Tachiki, Solid State Commun. **72**, 1183 (1989).
[13] S. Kohiki, S. Hayashi, H. Adachi, H. Hatta, K. Setsune, and K. Wasa, J. Phys. Soc. Jpn. **58**, 4139 (1989).
[14] A. Grassmann, J. Ströbel, M. Klauda, J. Schlötterer, and G. Saemann-Ischenko, Europhys. Lett. **9**, 827 (1989).
[15] A. Fujimori, Y. Tokura, H. Eisaki, H. Takagi, S. Uchida, and E. Takayama-Muromachi, Phys. Rev. B **42**, 325 (1990).
[16] T. Suzuki, M. Nagoshi, Y. Fukuda, K. Oh-ishi, Y. Syono, and M. Tachiki, Phys. Rev. B **42**, 4263 (1990).
[17] Y. Sakisaka, T. Maruyama, Y. Morikawa, H. Kato, K. Edamoto, M. Okusawa, Y. Aiura, H. Yanashima, T. Terashima, Y. Bando, K. Iijima, K. Yamamoto, and K. Hirata, Solid State Commun. **74**, 609 (1990); Phys. Rev. B **42**, 4189 (1990).
[18] J. W. Allen, C. G. Olson, M. B. Maple, J.-S. Kang, L. Z. Liu, J.-H. Park, R. O. Anderson, W. P. Ellis, J. T. Markert, Y. Dalichaouch, and R. Liu, Phys. Rev. Lett. **64**, 595 (1990).
[19] S. Kohiki, J. Kawai, T. Kamada, S. Hayashi, H. Adachi, K. Setsune, and K. Wasa, Solid State Commun. **73**, 787 (1990).
[20] S. Kohiki, J. Kawai, S. Hayashi, H. Adachi, H. Hatta, K. Setsune, and K. Wasa, J. Appl. Phys. **68**, 1229 (1990).
[21] M. Klauda, J. P. Ströbel, J. Schlötterer, A. Grassmann, J. Markl, and G. Saemann-Ischenko, Physica C **173**, 109 (1991).
[22] R. P. Vasquez, A. Gupta, and A. Kussmaul, Solid State Commun. **78**, 303 (1991).
[23] F. Parmigiani, L. E. Depero, T. Minerva, and J. B. Torrance, J. Electron Spectrosc. Relat. Phenom. **58**, 315 (1992).
[24] D. M. King, Z.-X. Shen, D. S. Dessau, B. O. Wells, W. E. Spicer, A. J. Arko, D. S. Marshall, J. DiCarlo, A. G. Loeser, C. H. Park, E. R. Ratner, J. L. Peng, Z. Y. Li, and R. L. Greene, Phys. Rev. Lett. **70**, 3159 (1993).
[25] R. O. Anderson, R. Claessen, J. W. Allen, C. G. Olson, C. Janowitz, L. Z. Liu, J.-H. Park, M. B. Maple, Y. Dalichaouch, M. C. de Andrade, R. F. Jardim, E. A. Early, S.-J. Oh, and W. P. Ellis, Phys. Rev. Lett. **70**, 3163 (1993).
[26] T. R. Cummins and R. G. Egdell, Phys. Rev. B **48**, 6556 (1993).
[27] N. L. Wang, K. Q. Ruan, Y. Chong, M. Deng, C. Y. Wang, Z. J. Chen, L. Z. Cao, J. X. Wu, and J. S. Zhu, Phys. Rev. B **51**, 3791 (1995).
[28] Y. Tokura, H. Takagi, and S. Uchida, Nature (London) **337**, 345 (1989).
[29] H. Takagi, S. Uchida, and Y. Tokura, Phys. Rev. Lett. **62**, 1197 (1989).
[30] M. Naito and H. Sato, Appl. Phys. Lett. **67**, 2557 (1995).
[31] H. Sato, M. Naito, S. Kinoshita, T. Arima, and Y. Tokura, Appl. Phys. Lett. **66**, 514 (1995).
[32] H. Sato and M. Naito, Physica C **274**, 221 (1997).
[33] H. M. Appelboom, H. Sato, and M. Naito, Physica C **221**, 125 (1994).
[34] The substrate size was typically 1/4 inch square.
[35] W. Jiang, S. N. Mao, X. X. Xi, X. Jiang, J. L. Peng, T. Venkatesan, C. J. Lobb, and R. L. Greene, Phys. Rev. Lett. **73**, 1291 (1994).
[36] J. S. Kim and D. R. Gaskell, Physica C **209**, 381 (1993).
[37] Y. Idemoto, K. Fueki, and M. Sugiyama, J. Solid State Chem. **92**, 489 (1991); Y. Idemoto, K. Uchida, and K. Fueki, Physica C **222**, 333 (1994).
[38] M. Scavini, G. Chiodelli, G. Spinolo, and G. Flor, Physica C **230**, 412 (1994).
[39] At a distance of 8 cm.
[40] R. L. Kurtz, R. Stockbauer, T. E. Madey, D. Mueller, A. Shih, and L. Toth, Phys. Rev. B **37**, 7936 (1988).
[41] R. L. Kurtz, S. W. Robey, R. L. Stockbauer, D. Mueller, A. Shih, and L. Toth, Phys. Rev. B **39**, 4768 (1989).
[42] J. J. Yeh and I. Lindau, At. Data Nucl. Data Tables **32**, 1 (1985).
[43] RHEED patterns (not shown here) suggest that, in the films oxygenated by ozone gas, some excess oxygen atoms may occupy interstitial sites other than O(3) at the surface.
[44] P. G. Radaelli, J. D. Jorgensen, A. J. Schultz, J. L. Peng, and R. L. Greene, Phys. Rev. B **49**, 15 322 (1994).
[45] A. J. Schults, J. D. Jorgensen, J. L. Peng, and R. L. Greene, Phys. Rev. B **53**, 5157 (1996).
[46] P. Ghigna, G. Spinolo, A. Filipponi, A. V. Chadwick, and P. Hanmer, Physica C **246**, 345 (1995).
[47] E. Moran, A. I. Nazzal, T. C. Huang, and J. B. Torrance, Physica C **160**, 30 (1989).
[48] Both of the films show very sharp streaks in the zeroth Laue zone, which contain bulk diffraction and superstructure diffraction with three times periodicity, and also show faint streaky spots in the first Laue zone.
[49] C. Marin, J. Y. Henry, and J. X. Boucherle, Solid State Commun. **86**, 425 (1993).
[50] The surfaces of the present NCCO films were found to be significantly more stable to the atmosphere than those in the previous reports (e.g., see Ref. 22), probably due to the superiority in crystalline quality of the present MBE-grown films [H. Yamamoto, M. Naito, and H. Sato (unpublished)].
[51] Q. Huang, J. F. Zasadzinski, N. Tralshawala, K. E. Gray, D. G. Hinks, J. L. Peng, and R. L. Greene, Nature (London) **347**, 369 (1990).